HAL
open science

Benchmark on the 3D Numerical Modeling of a Superconducting Bulk

Kévin Berger, Loïc Quéval, Abelin Kameni, Lotfi Alloui, Brahim Ramdane, Frédéric Trillaud, Ludovic Makong Hell, Gérard Meunier, Philippe Masson, Jean Lévêque

To cite this version:

Kévin Berger, Loïc Quéval, Abelin Kameni, Lotfi Alloui, Brahim Ramdane, et al.. Benchmark on the 3D Numerical Modeling of a Superconducting Bulk. 2016. hal-01548728v1

HAL Id: hal-01548728

https://hal.science/hal-01548728v1

Preprint submitted on 28 Jun 2017 (v1), last revised 15 Nov 2017 (v4)

HAL is a multi-disciplinary open access archive for the deposit and dissemination of scientific research documents, whether they are published or not. The documents may come from teaching and research institutions in France or abroad, or from public or private research centers.

L'archive ouverte pluridisciplinaire **HAL**, est destinée au dépôt et à la diffusion de documents scientifiques de niveau recherche, publiés ou non, émanant des établissements d'enseignement et de recherche français ou étrangers, des laboratoires publics ou privés.

Benchmark on the 3D Numerical Modeling of a Superconducting Bulk

Kévin Berger[1], Loïc Quéval[2], Abelin Kameni[2], Lotfi Alloui[2,3], Brahim Ramdane[4], Frédéric Trillaud[5], Ludovic Makong Hell[2,6], Gérard Meunier[4], Philippe Masson[6], Jean Lévêque[1]

[1] GREEN, Université de Lorraine, 54506 Vandœuvre-lès-Nancy, France
[2] Group of electrical engineering - Paris (GeePs), CNRS UMR 8507, CentraleSupélec, UPSud, UPMC, Gif-sur-Yvette, France
[3] Laboratoire de Modélisation des Systèmes Energétiques LMSE, Université de Biskra, BP 145, 07000 Biskra, Algeria
[4] University Grenoble Alpes / CNRS, G2Elab, 38042 Grenoble, France
[5] Instituto de Ingenieria, Universidad Nacional Autonoma de Mexico, CDMX, 04510 Mexico
[6] University of Houston, Houston, TX, USA

So far, various numerical models have been developed to simulate high temperature superconductor in 3D. However, the lack of analytical solutions in the 3D case and the scarcity of experimental data make it difficult to evaluate the accuracy of the proposed models. In the present work, a benchmark on the 3D numerical modeling of a superconducting bulk is introduced. The problem is tackled by 5 independent teams using 6 different numerical models. After a detailed description of the models and their implementations, the results obtained are compared and discussed.

***Index Terms*— 3D modeling, AC losses, FEM, FVM, high temperature superconductors.**

I. Introduction

High Temperature Superconductors (HTS) are promising for applications requiring high power densities, e.g. superconducting motors [1] or bearings [2]. Driven by practical and commercial applications, various numerical models have been developed to simulate 2D and 3D problems involving HTS [3]. Most of them have been developed to assess the AC losses in thin wires and tapes. Indeed AC losses are one of the key factors to size properly the cryogenic system [4].

Different formulations have been proposed to deal with the nonlinearity of superconductors. The most popular one is probably the **H**-formulation [5]–[8]. But others formulations have been used too such as **A**-V and **T**-Ω [9]–[11]. The latter formulation proved to be more suitable to model 3D eddy current problems due to a better numerical stability and convergence even though the former may lead to a smaller problem to solve [12]. In addition, mixed and alternative formulations as well as topological approach have also been considered [13]–[16].

These formulations were readily available or have been implemented or modified to incorporate the nonlinearity of the superconducting material in various softwares. The following commercial finite element method (FEM) softwares have been used to model superconductors: ANSYS, Opera-3D, Flux2D, Flux3D, COMSOL Multiphysics and FlexPDE [17]–[21]. Alternatively, open-source FEM codes have been tried out with a special mention of ONELAB and FreeFem++ [22], [23]. It should be noted that even though FEM has proved to be a powerful method to carry out modeling of superconductors, other approaches have been developed based on finite difference method, finite volume method, variational principle or integral methods either to cross-check results or as an alternative approach to lower the computational load [24]–[27]. In this vast pool of options tackling diverse problems, it is difficult to point out the advantages and disadvantages of one method compared to the other.

Over the years, partial attempts to address this issue have been conducted [11]. The present work is a step further in that direction. Methods and formulations used by 5 independent teams involved in HTS numerical modeling are compared on the specific problem of the magnetization of a superconducting cube [28], [29]. This problem is of interest because of the specific current density distribution that may be induced in the cube.

In section II, we describe in details the benchmark problem. Section III gives an overview of the numerical models used by the different teams. The main results are summarized in section IV: the AC losses in partial and complete penetrations, and the current density distributions.

II. Benchmark Model

A. Geometry

The geometry is a superconducting cube having an edge length d of 10 mm. The cube is surrounded by a 100 mm box of air, as shown in Fig. 1.

B. Material properties

The electrical behavior of the superconductor is modeled with a power law linking the electrical field **E** to the current density **J** as:

$$\mathbf{E} = \frac{E_c}{J_c}\left(\frac{\|\mathbf{J}\|}{J_c}\right)^{n-1}\mathbf{J} \text{ with } \|\mathbf{J}\| = \sqrt{J_x^2 + J_y^2 + J_z^2} \qquad (1)$$

The parameters $J_c = 2.5\times10^6$ A/m^2 and $n = 25$ have been chosen close to values obtained from experimental characterization on cylindrical Bi-2223 samples with $E_c = 1$ μV/cm [30]. This opens the possibility to perform later experiments to validate this benchmark. The magnetic property of the superconductor can be fully described by the nonlinear

dependence of its electrical resistivity upon current which is directly inferred form the power law. Therefore, it is sensible to use the magnetic permeability of vacuum μ_0 to describe the **B**-**H** curve for magnetic flux densities ranging from a few milli-Tesla, corresponding to the lower critical magnetic field, to the upper critical magnetic field of type-II superconductors.

C. Case studies

A uniform sinusoidal external magnetic flux density $B_a(t)$ of amplitude B_{max}, and frequency 50 Hz, is applied to the cube along the z axis.

The full penetration flux density B_p can be estimated according to $B_p = \mu_0 J_c d / 2 = 15.7$ mT [31]. Two cases will be therefore investigated:

- Partial penetration: $B_{max} = 5$ mT $< B_p$. In this case, a current-free region exists in the center of the superconductor region.
- Complete penetration: $B_{max} = 20$ mT $> B_p$. In this case, the current penetrates the entire superconductor region.

The global variable of interest is the instantaneous AC losses p_{AC}:

$$p_{AC}(t) = \iiint_{\text{HTS cube}} \mathbf{E} \cdot \mathbf{J} \, dv \tag{2}$$

and the steady-state average AC losses P computed as [8]:

$$P = \frac{2}{T} \int_{T/2}^{T} p_{AC}(t) \, dt \tag{3}$$

III. Numerical Models

A. General description

Table I summarizes the methods, the formulations, the software and the contributors for each numerical model.

TABLE I
NUMERICAL MODELS

Label	Method	Formulation	Software / Code	Task leader
(B.1)	FEM	**H**	Daryl-Maxwell	B. Ramdane & G. Escamez
(B.2)	FEM	**H**	COMSOL(1)	K. Berger
(B.3)	FEM	**H**	COMSOL(2)	K. Berger
(B.4)	FEM	**H**	COMSOL(3)	L. Quéval
(B.5)	FEM	**H**	GetDP	A. Kameni
(B.6)	FVM	**A**-V	MATLAB	L. Alloui

In COMSOL 5.0, the **H**-formulation can be implemented: (1) by using the available mfh physics, (2) by substituting **H** into **A** in the **A** formulation of the mf physics, (3) by manually implementing the differential equations with the pde physics.

Daryl-Maxwell is a homemade FEM software developed at Polytechnique Montréal. It is devised specifically for solving large 3D nonlinear electromagnetic problems in the time domain. It was initially developed to tackle problems involving superconductors [32] and ferromagnetic materials. Daryl-Maxwell uses an **H**-formulation with fixed and/or adaptive time stepping.

COMSOL Multiphysics is a commercial multiphysics FEM software [18]. In the superconductor modeling community, it has been intensively used for 2D and 3D modeling of superconductors, mainly using the **H**-formulation implemented with the PDE physics [7], [8], [33]–[35]. It provides only adaptive time stepping for the temporal resolution with little control on the minimum time step, which can lead to long computation times especially in 3D.

GetDP is an open-source finite element solver using mixed elements to solve partial differential equations in 1D, 2D and 3D. The computation of AC losses in superconductors has been recently reported [36].

The Finite Volume Method (FVM) can be regarded as a special version of the weighted residuals method. It consists in dividing the domain into a number of non-overlapping subdomains or control volumes such that there is one control volume surrounding each computing node. The weighting function is setting to be unity over one subdomain and zero everywhere else. This method proved to be numerically stable in the case of highly nonlinear problems. For this reason, this approach has been implemented in a 3D computation code, under the MATLAB environment, dedicated mainly to solving electromagnetic problems with superconducting materials [24].

B. Mesh

Simulations have been carried out using the same reference mesh for the models (B.1)-(B.4). It consists of 27 982tetrahedrons with 8 688 tetrahedrons in the HTS cube region, which leads to 33 612 DOF for 1st order elements. It was chosen as the best compromise between the estimated AC losses and the computation. Fig. 1 shows the mesh (left) with the HTS cube at the center and its quality in a y-z cut-plane at $x = 0$ (right).

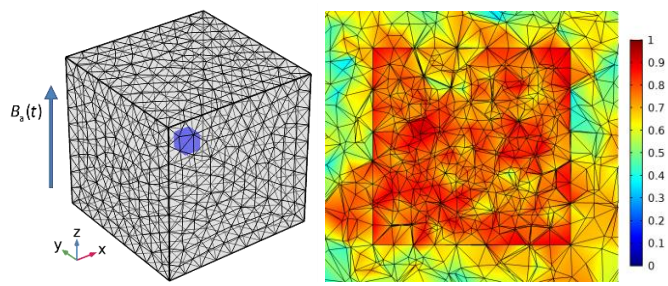

Fig. 1. (left) Mesh with the HTS cube at the center. (right) Quality of the mesh in a y-z cut-plane at $x = 0$.

Due to tag identification problems, the mesh used in GetDP (B.5) has been built with Gmsh [37]. Because the solver is very sensitive to the quality of the mesh and its size, a mesh denser than the reference mesh was selected. This mesh has been optimized to get the best results in a reasonable computation time. It consists of a total of 59 617 tetrahedrons with 25 930 tetrahedrons in the HTS cube.

The FVM used by (B.6) uses a cubic mesh with 20 elements per edge of the HTS cube which leads to 8 000 hexahedrons in the superconducting domain.

C. Technical information about the methods

Table II summarizes the methods used for each model. Note that:

- All methods used an implicit time discretization scheme,
- FEM methods are based on edge elements (Nédélec) of order 1,
- (B.1) uses PARDISO as direct solver and fixed time steps but a variant of DASSL is also possible.
- In COMSOL, absolute and relative tolerances have been set at 10^{-3} and 10^{-6}, respectively.

TABLE II
METHODS USED FOR EACH NUMERICAL MODEL

	(B.1)	(B.2)	(B.3)	(B.4)	(B.5)	(B.6)
Time dependent solver DASPK			X	X		
Fixed time steps	X				X	X
Direct solver MUMPS		X	X	X	X	
Direct solver PARDISO	X					
Gauss Seidel iterative method						X
Newton Raphson method		X	X	X	X	

D. Treatment of the non-linearity arising from E(J)

All **H**-formulations except (B.3) solve:

$$\mu_0 \frac{\partial \mathbf{H}}{\partial t} + \nabla \times \left(\rho(\mathbf{J}) \nabla \times \mathbf{H} \right) = 0 \text{ with } \rho(\mathbf{J}) = \frac{E_c}{J_c} \left(\frac{\|\mathbf{J}\|}{J_c} \right)^{n-1} \quad (4)$$

Since (B.3) is based on an **A** formulation where $\mathbf{A} \rightarrow \mathbf{H}$, then $\sigma \rightarrow \mu$ and $\mu \rightarrow \sigma$. Consequently, $\sigma(\mathbf{J})$ is needed as an input of the model and not $\rho(\mathbf{J})$. In order to avoid instabilities when the conductivity of the HTS material tends to infinity, corresponding to the case of null current density, the following expression was used:

$$\sigma(\mathbf{J}) = \left(\frac{E_c}{J_c} \left(\frac{\|\mathbf{J}\|}{J_c} \right)^{n-1} + \rho_0 \right)^{-1} \text{ with } \rho_0 = 10^{-14}\ \Omega \cdot \mathrm{m} \quad (5)$$

To avoid the evaluation of zero at a negative power in COMSOL, (B.3) and (B.4) computed the norm of current density using:

$$\|\mathbf{J}\| = \sqrt{J_x^2 + J_y^2 + J_z^2 + \varepsilon} \text{ with } \varepsilon = 2.22 \times 10^{-16}\ \mathrm{A}^2 \cdot \mathrm{m}^{-4} \quad (6)$$

The **A**-V formulation employed by (B.6) involves a Coulomb gauge (div **A** = 0) and the conservation of the current density (div **J** = 0) which leads to the following set of equations:

$$\left\{ \begin{array}{l} \nabla \times \left(\mu_0^{-1} \nabla \times \mathbf{A} \right) - \nabla \left(\mu_0^{-1} \nabla \cdot \mathbf{A} \right) + \sigma(\mathbf{E}) \left(\frac{\partial \mathbf{A}}{\partial t} + \nabla V \right) = 0 \\ \nabla \cdot \left(-\sigma(\mathbf{E}) \left(\frac{\partial \mathbf{A}}{\partial t} + \nabla V \right) \right) = 0 \end{array} \right\} \quad (7)$$

$$\text{with } \sigma(\mathbf{E}) = \left(\frac{E_c}{J_c} \left(\frac{\|\mathbf{E}\|}{E_c} \right)^{(n-1)/n} + \rho_0 \right)^{-1} \quad (8)$$

The conductivity of the HTS material is also required but the function is different, indeed (B.6) uses $\sigma(\mathbf{E})$ compared to $\sigma(\mathbf{J})$ for (B.3). Previous studied have shown that the use of $\sigma(\mathbf{E})$ made the convergence of the solver much more difficult [18], [38].

To ensure the stability and convergence of the solver, (B.5) requires a linearization at each time step of the nonlinear function in (4) which is achieved as shown in [39].

IV. RESULTS AND DISCUSSION

A. AC losses

The instantaneous AC losses p_{AC} for partial and complete penetration cases, are shown in Fig. 2. Since these calculations are based on a time transient nonlinear simulation with a superconductor initially in a virgin state, it is necessary to run the simulation until the initial transient dies out and the steady state is established. In the present cases, the steady state regime is reached after half a period. The results of the different numerical models are in good agreement with each other with the exception of (B.6). One can see a slight overshoot, for the partial penetration case, of the instantaneous losses at the maximum value with some discrepancies during the increasing portion of the losses. The **A**-V formulation presents additional challenges compared to the **H**-formulation especially in terms of convergence and stability.

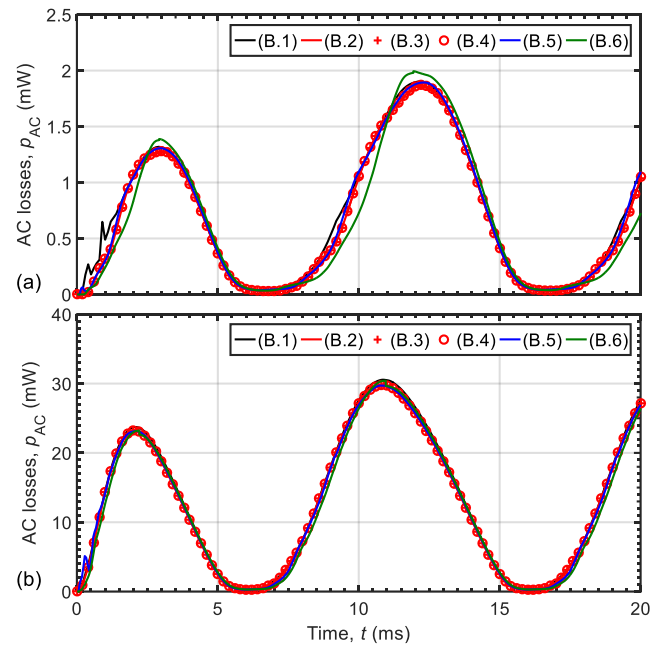

Fig. 2. Instantaneous AC losses p_{AC} for the six different models with (a) B_{max} = 5 mT and (b) B_{max} = 20 mT.

When the applied field amplitude increases, we can notice that the instantaneous AC losses peaks shift towards t = T/2 and t = T, corresponding to the moment when the derivative of the applied field is maximum.

The average AC losses P and the computation times are given in Table III. Values of losses are below 1 mW for B_{max} = 5 mT, while they grow up to 13 mW for B_{max} = 20 mT. While the instantaneous AC losses predicted by (B.6) were different from the other models, the average AC losses are similar due to the integration (3). Choosing (B.3) as the reference, the maximum deviation is 5.8 % and 10.2 % for B_{max} = 5 mT and 20 mT, respectively. Although the results are very similar, these values reflect clearly some discrepancies arising from differences in the implementation of the methods.

TABLE III
COMPUTING TIME AND AC LOSSES

Label	B_{max} = 5 mT		B_{max} = 20 mT	
	Comp. time	P (mW)	Comp. time	P (mW)
(B.1)	(1) 134 min 00 s	0.8354	(1) 318 min 00 s	14.3399
(B.2)	(2) 42 min 20 s	0.7933	(2) 931 min 38 s	13.0074
(B.3)	**(2) 6 min 39 s**	**0.7933**	**(2) 10 min 55 s**	**13.0090**
(B.4)	(2) 11 min 06 s	0.7969	(2) 17 min 17 s	13.0088
(B.5)	-	0.8396	-	13.9087
(B.6)	-	0.8303	-	13.8453

The computers used are: (1) Intel® Core™ i5-2540M CPU @ 2.60 GHz (Turbo Boost 3.30 GHz), 8 GB RAM, Mac OS X 10.10, and (2) Intel® Core™ i7-6700 CPU @ 3.40 GHz (Turbo Boost 4.00 GHz), 32 GB RAM, Windows 7 64 bits.

(B.3) seems to be the fastest model. It is interesting to notice that methods (B.2), (B.3) and (B.4) use the same software with exactly the same solvers settings and tolerances. However, (B.2) is six times faster than (B.3). This is surprising because (B.2) is the formulation proposed by COMSOL for solving problems with superconductors since the version 4.3b. This is probably the reason why (B.4) is still widely being used.

Fig. 3 shows the solver outputs of (B.2) with the number of iterations (a) and the stepsize taken by the adaptive solver (b). We observe that the higher the number of iterations, the smaller the stepsize, which leads to large computing times. Excluding the transient, the stepsize of (B.2) are roughly 20 times larger than the ones observed with (B.3) and (B.4) with 5 times more iterations. This explains the differences in computing times reported in Table III between (B.2) and (B.3) but not between (B.3) and (B.4).

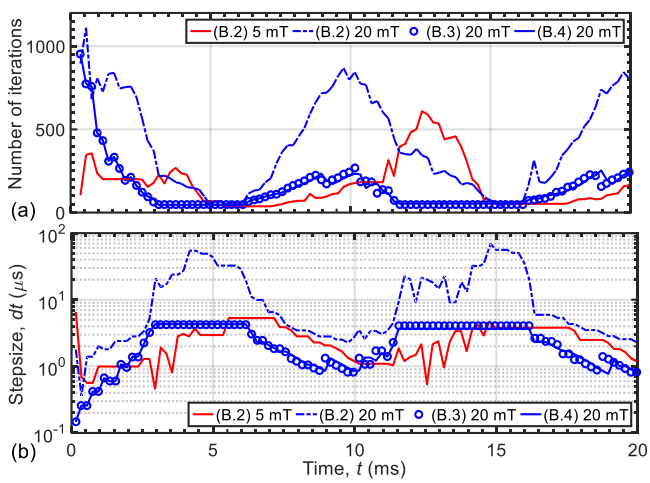

Fig. 3. (a) Number of iterations vs. time and (b) stepsize taken by the adaptive solvers (B.2)-(B.4).

B. Current density

Fig. 4 shows the normalized current density J_x / J_c from (B.3) at $t = 15$ ms for the partial penetration (left) and the complete penetration case (right). The y-z cut planes used for the representation are located at $x/d = \pm 1/3$ and $x = 0$. The induced currents are flowing in closed square loops in a plane perpendicular to the applied field. In a conventional ohmic conductor, the current loops would be more circular close to the center of the cube. This particularity of superconductors is due to the nonlinear relationship between **E** and **J**. This phenomenon has been seen from the magneto-optic images performed on thin films [40].

Another particular feature of superconductors is that the induced currents flow with a non-zero J_z component close to the corners of the cube. This J_z component is a consequence of the self-field that, for square loops of current, is higher near the corners. This tends to bend the current lines as shown with the streamlines in Fig. 4 (left). The current flowing in square loops cannot fully cancel the self-field that is canceled thanks to the J_z components. For applied fields well above the penetration field, the self-field is not relevant, and the J_z components tend towards zero everywhere. This explanation is consistent with those given in [41].

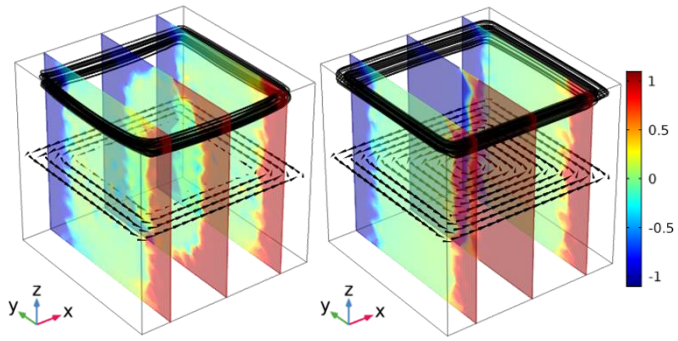

Fig. 4. Normalized current density J_x / J_c from (B.3) at $t = 15$ ms for $B_{max} = 5$ mT (left) and 20 mT (right). y-z cut planes are located at $x/d = \pm 1/3$ and $x = 0$. The current flows following the shape of the borders as shown with the cones in the x-y plane at $z = 0$.

V. Conclusion and Perspectives

A benchmark on 3D superconductor modeling has been proposed. It has been solved using 6 different numerical models developed by 5 independent teams. The results show good agreement between the models when considering the AC losses, despite large difference in terms of computational load. The **A**-V formulation generally presents greater numerical challenges than the **H**-formulation in terms of convergence and stability. The comparison of a model implemented using the open-source code GetDP with other commonly used models is a significant contribution of this article. Explanations have been proposed to clarify the square shape of current loops observed in the HTS cube, and the existence of the J_z component near the corner of the cube.

In addition to **A**-V and **T**-Ω formulation finite element models, alternative models such as stochastic models could be considered later.

References

[1] H. Matsuzaki *et al.*, "An axial gap-type HTS bulk synchronous motor excited by pulsed-field magnetization with vortex-type armature copper windings," *IEEE Transactions on Applied Superconductivity*, vol. 15, no. 2, pp. 2222–2225, Jun. 2005.

[2] H. Walter *et al.*, "First Heavy Load Bearing for Industrial Application with Shaft Loads up to 10 kN," *Journal of Physics: Conference Series*, vol. 43, no. 1, p. 995, 2006.

[3] M. D. Ainslie and H. Fujishiro, "Modelling of bulk superconductor magnetization," *Superconductor Science and Technology*, vol. 28, no. 5, p. 53002, 2015.

[4] F. Grilli, "Numerical modelling of HTS applications," *IEEE Transactions on Applied Superconductivity*, vol. 26, no. 3, p. 0500408, 2016.

[5] R. Brambilla, F. Grilli, and L. Martini, "Development of an edge-element model for AC loss computation of high-temperature superconductors," *Superconductor Science and Technology*, vol. 20, pp. 16–24, 2007.

[6] M. Zhang and T. A. Coombs, "3D modeling of high- T c superconductors by finite element software," *Supercond. Sci. Technol.*, vol. 25, no. 1, p. 015009, 2012.

[7] V. M. R. Zermeño and F. Grilli, "3D modelling and simulation of 2G HS stacks and coils," *Superconductor Science and Technology*, vol. 27, p. 044025 (7pp), 2014.

[8] L. Quéval, V. M. R. Zermeño, and F. Grilli, "Numerical models for ac loss calculation in large-scale applications of HTS coated conductors," *Superconductor Science and Technology*, vol. 29, p. 024007 (10pp), 2016.

[9] A. Henning, M. Lindmayer, and M. Kurrat, "Simulation Setup for Modeling the Thermal, Electric, and Magnetic Behavior of High Temperature Superconductors," *Physics Procedia*, vol. 36, pp. 1195–1205, 2012.

[10] S. Pratap and C. S. Hearn, "3-D Transient Modeling of Bulk High-Temperature Superconducting Material in Passive Magnetic Bearing

Applications," *IEEE Transactions on Applied Superconductivity*, vol. 25, no. 5, p. 5203910 (10pp), 2015.

[11] S. Stavrev *et al.*, "Comparison of Numerical Methods for Modeling of Superconductor," *IEEE Transactions on Magnetics*, vol. 38, no. 2, pp. 849–852, 2002.

[12] F. Grilli *et al.*, "Finite-Element Method Modeling of Superconductors: From 2-D to 3-D," *IEEE Transactions on Applied Superconductivity*, vol. 15, no. 1, pp. 17–25, 2005.

[13] T. Yanagawa, K. Kaneda, A. Ishiyama, S. Noguchi, and H. Yamashita, "A new analysis method for accurate supercurrent distribution inside high-temperature superconducting bulk," *IEEE Transactions on Magnetics*, vol. 42, no. 4, pp. 751–754, 2006.

[14] H. Zhang, M. Zhang, and W. Yuan, "An efficient 3D finite element method model based on the T–A formulation for superconducting coated conductors," *Superconductor Science and Technology*, vol. 30, p. 024005 (7pp), 2017.

[15] K. Berger, J. Lévêque, D. Netter, B. Douine, and A. Rezzoug, "Influence of Temperature and/or field dependencies of the E-J power law on Trapped magnetic field in bulk YBaCuO," *IEEE Transactions on Applied Superconductivity*, vol. 17, no. 2, pp. 3028–3031, 2007.

[16] V. Lahtinen, M. Lyly, A. Stenvall, and T. Tarhasaari, "Comparison of three eddy current formulations for superconductor hysteresis loss modelling," *Superconductor Science and Technology*, vol. 25, p. 115001 (14pp), 2012.

[17] F. Sirois and F. Grilli, "Potential and limits of numerical modelling for supporting the development of HTS devices," *Superconductor Science and Technology*, vol. 28, p. 043002 (13pp), 2015.

[18] M. Costa *et al.*, "3D Modeling of Coupling Between Superconducting Filaments via Resistive Matrix in AC Magnetic Field," *IEEE Transactions on Applied Superconductivity*, vol. 13, no. 2, pp. 3634 – 3637, 2003.

[19] Y. Zhilichev, "Simulation of Critical Currents in Bulk Superconductors by Modified FEA and Hybrid Methods," *IEEE Transactions on Applied Superconductivity*, vol. 27, no. 4, p. 0600105 (5pp), 2017.

[20] J. Grundmann, M. Lindmayer, R. Röckelein, and W. Schmidt, "Simulation of HTS switching with the finite element analysis program ANSYS," *Superconductor Science and Technology*, vol. 16, pp. 562–565, 2003.

[21] A. M. Campbell, "Solving the critical state using flux line properties," *Superconductor Science and Technology*, vol. 27, p. 124006 (10pp), 2014.

[22] G. P. Lousberg, M. Ausloos, C. Geuzaine, P. Dular, P. Vanderbemden, and B. Vanderheyden, "Numerical simulation of the magnetization of high-temperature superconductors: a 3D finite element method using a single time-step iteration," *Superconductor Science and Technology*, vol. 22, p. 055005 (9pp), 2009.

[23] V. M. R. Zermeño, F. Sirois, M. Takayasu, M. Vojenciak, A. Kario, and F. Grilli, "A self-consistent model for estimating the critical current of superconducting devices," *Superconductor Science and Technology*, vol. 28, p. 085004 (12pp), 2015.

[24] L. Alloui, F. Bouillault, L. Bernard, J. Lévêque, and S. M. Mimoune, "3D modeling of forces between magnet and HTS in a levitation system using new approach of the control volume method based on an unstructured grid," *Physica C: Superconductivity and its Applications*, vol. 475, pp. 32–37, 2012.

[25] G. J. Barnes, D. Dew-Hughes, and M. D. McCulloch, "Finite difference modelling of bulk high temperature superconducting cylindrical hysteresis machines," *Superconductor Science and Technology*, vol. 13, pp. 229–236, 2000.

[26] M. L. Khene, L. Alloui, F. Bouillault, A. Kameni Ntichi, and S. M. Mimoune, "3-D Numerical Evaluation of Trapped Magnetic Field and Temperature of a Rectangular GdBaCuO Bulk Magnetized by MMPSC Method," *IEEE Transactions on Magnetics*, vol. 51, no. 3, p. 9000204 (4pp), 2015.

[27] E. Pardo and M. Kapolka, "3D computation of non-linear eddy currents: Variational method and superconducting cubic bulk," *Journal of Computational Physics*, vol. 344, pp. 339–363, 2017.

[28] A. Kameni, M. Boubekeur, L. Alloui, F. Bouillault, J. Lambretchs, and C. Geuzaine, "A 3-D Semi-Implicit Method for Computing the Current Density in Bulk Superconductors," *IEEE Transactions on Magnetics*, vol. 50, no. 2, p. 7009204 (4pp), 2014.

[29] E. Pardo and M. Kapolka, "3D magnetization currents, magnetization loop, and saturation field in superconducting rectangular prisms," *Superconductor Science and Technology*, vol. 30, p. 064007 (11pp), 2017.

[30] K. Berger, J. Leveque, D. Netter, B. Douine, and A. Rezzoug, "AC transport losses calculation in a Bi-2223 current lead using thermal coupling with an analytical formula," *IEEE Transactions on Applied Superconductivity*, vol. 15, no. 2, pp. 1508–1511, Jun. 2005.

[31] D. -X. Chen and R. B. Goldfarb, "Kim model for magnetization of type-II superconductors," *Journal of Applied Physics*, vol. 66, no. 6, pp. 2489–2500, Sep. 1989.

[32] G. Escamez, F. Sirois, A. Badel, G. Meunier, B. Ramdane, and P. Tixador, "Numerical impact of using different E-J relationships for 3-D simulations of AC losses in MgB2 superconducting wires," *IEEE Transactions on Magnetics*, vol. 52, no. 3, p. 7402904 (4pp), 2016.

[33] COMSOL, "COMSOL Multiphysics® Modeling Software." [Online]. Available: http://www. comsol.com/. [Accessed: 22-Jun-2017].

[34] V. M. R. Zermeño, F. Grilli, and F. Sirois, "A full 3D time-dependent electromagnetic model for Roebel cables," *Superconductor Science and Technology*, vol. 26, p. 052001 (8pp), 2013.

[35] Z. Hong, W. Yuan, M. Ainslie, Y. Yan, R. Pei, and T. A. Coombs, "AC Losses of Superconducting Racetrack Coil in Various Magnetic Conditions," *IEEE Transactions on Applied Superconductivity*, vol. 21, no. 3, pp. 2466–2469, Jun. 2011.

[36] C. Geuzaine, A. Kameni, and A. Stenvall, "Superconducting wire - ONELAB." [Online]. Available: http://onelab.info/wiki/Superconducting_wire. [Accessed: 22-Jun-2017].

[37] C. Geuzaine and J.-F. Remacle, "Gmsh - A three-dimensional finite element mesh generator with built-in pre- and post-processing facilities." [Online]. Available: http://gmsh.info/. [Accessed: 22-Jun-2017].

[38] E. Vinot, "Modélisation des supraconducteurs HTC Applications au calcul des pertes AC," Institut National Polytechnique de Grenoble - INPG, 2000.

[39] A. Kameni, J. Lambrechts, J. F. Remacle, S. Mezani, F. Bouillault, and C. Geuzaine, "Discontinuous Galerkin Method for Computing Induced Fields in Superconducting Materials," *IEEE Transactions on Magnetics*, vol. 48, no. 2, pp. 591–594, Feb. 2012.

[40] C. Jooss, J. Albrecht, H. Kuhn, S. Leonhardt, and H. Kronmüller, "Magneto-optical studies of current distributions in high-Tc superconductors," \iRep. Prog. Phys., vol. 65, no. 5, p. 651, 2002.

[41] E. Pardo and M. Kapolka, "3D computation of non-linear eddy currents: Variational method and superconducting cubic bulk," *Journal of Computational Physics*, vol. 344, pp. 339–363, 2017.